Photolysis of Caged Calcium in Femtoliter Volumes Using Two-Photon Excitation

Edward B. Brown,*# Jason B. Shear,¶ Stephen R. Adams,‖ Roger Y. Tsien,‖** and Watt W. Webb*§

*Developmental Resource for Biophysical Imaging and Optoelectronics, #Department of Physics, and §Department of Applied and Engineering Physics, Cornell University, Ithaca, New York 14853; ¶Department of Chemistry and Biochemistry, University of Texas, Austin, Texas 78712; and ‖Department of Pharmacology and **Howard Hughes Medical Institute, University of California, La Jolla, California 92093-0647 USA

ABSTRACT A new technique for the determination of the two-photon uncaging action cross section (δ_u) of photolyzable calcium cages is described. This technique is potentially applicable to other caged species that can be chelated by a fluorescent indicator dye, as well as caged fluorescent compounds. The two-photon action cross sections of three calcium cages, DM-nitrophen, NP-EGTA, and azid-1, are studied in the range of excitation wavelengths between 700 and 800 nm. Azid-1 has a maximum δ_u of ~1.4 GM at 700 nm, DM-nitrophen has a maximum δ_u of ~0.013 GM at 730 nm, and NP-EGTA has no measurable uncaging yield. The equations necessary to predict the amount of cage photolyzed and the temporal behavior of the liberated calcium distribution under a variety of conditions are derived. These equations predict that by using 700-nm light from a Ti:sapphire laser focused with a 1.3-NA objective, essentially all of the azid-1 within the two-photon focal volume would be photolyzed with a 10-μs pulse train of ~7 mW average power. The initially localized distributions of free calcium will dissipate rapidly because of diffusion of free calcium and uptake by buffers. In buffer-free cytoplasm, the elevation of the calcium concentration at the center of the focal volume is expected to last for ~165 μs.

INTRODUCTION

The development of photolyzable chelators ("cages") and a new generation of calcium-sensitive dyes in the 1980s and 1990s has increased the spatial and temporal resolution of cellular calcium studies over whole cell techniques and consequently has provided new opportunities for determining the role of Ca^{2+} in cellular regulation and second-messenger signaling (Kao and Adams, 1993; Kaplan, 1990; Lipp et al., 1996). Calcium cages chemically react irreversibly after absorption of a UV photon to drastically increase the rate constant for release of Ca^{2+} (k_{off}) from the cage. The k_{off} for photolytically modified cages can be $\sim 10^5$ s^{-1} for some species (Ellis-Davies et al., 1996), thus providing a means of controlling cellular chemistry with a temporal resolution sufficient to mediate a wide range of cellular events. Calcium uncaging with a focused UV laser beam provides a diffraction-limited focal spot as small as 0.2 μm (e^{-2} radius) at the focal plane; unfortunately, the axial resolution of the UV excitation is relatively poor. If a series of slices is envisioned running through the double cone of focused illumination parallel to the focal plane and at varying distances from it, the same total amount of cage excitation will be generated in each slice. This results in calcium release throughout elongated regions within cells. Consequently, the spatial resolution of conventional uncaging techniques is limited to an approximately cylindrical region of the cell (McCray and Trentham, 1989). This spatial resolution for calcium uncaging is often inadequate for probing the properties of cellular microdomains, particularly in thicker cell regions.

True three-dimensionally resolved excitation of molecular chromophores can be achieved by using nonlinear (multiphoton) excitation. Two-photon excitation (2PE) requires the nearly simultaneous absorption of two photons to excite a chromophore. Consequently, the average rate of excitation per molecule, neglecting saturation, is given by

$$\text{Rate} \equiv \tfrac{1}{2}\delta\langle I^2\rangle \quad (1)$$

where δ is the two-photon absorption cross section in units of $cm^4 s$ $photon^{-1}$ (10^{-50} $cm^4 s$ $photon^{-1}$ equals 1 GM, or Göppert-Mayer), and $\langle I^2\rangle$ is the time average of the square incident local intensity in units of photons cm^{-2} s^{-1}. Once excited, a calcium cage releases calcium with a quantum yield of q, and the action cross section of the cage is given by $\delta_u \equiv q\delta$. Under nonsaturating conditions, the dependence of two-photon excitation on intensity squared gives the technique an intrinsic 3D resolution, with 80% of the excitation confined to the focal volume delineated by the e^{-2} isophotes of the focused laser intensity distribution (Denk et al., 1995). Using 2PE with high numerical aperture (NA) objectives and diffraction-limited focal volumes, release of calcium from molecular cages can be confined to less than femtoliter volumes, with ~1 μm resolution along the laser propagation axis (Denk, 1994).

This three-dimensionally resolved calcium release promises to be highly useful in studies of a variety of cellular processes, including calcium buffering. The kinetics of cellular calcium buffering dictate the time and length scales over which calcium can act as a second messenger in the

Received for publication 15 December 1997 and in final form 14 September 1998.

Address reprint requests to Dr. Watt Webb, Cornell University, Department of Applied and Engineering Physics, Clark Hall, Ithaca, NY 14853. Tel.: 607-255-3331; Fax: 607-255-7658; E-mail: ww2@cornell.edu.

0006-3495/99/01/489/11 $2.00

control of activities such as secretion and muscle contraction (Allbritton et al., 1992; Stern, 1992). Important work has been done in the exploration of these buffering kinetics, but these studies have been limited to whole-cell spatial resolution (T. Xu et al., 1997; Zhou and Neher, 1993). The local nature of stimulus-secretion coupling (Augustine and Neher, 1992) suggests that local buffering effects may play an important role in this cellular process and that three-dimensionally resolved measurement of calcium buffering kinetics would be an important application of two-photon calcium uncaging.

Another promising area for the application of 2PE calcium uncaging is in the study of the so-called sparking cells. Spontaneous localized transients of elevated calcium concentration, known as calcium "sparks," have been observed in mature skeletal, cardiac, and smooth muscle cells (Klein et al., 1996; Cheng et al., 1993; Nelson et al., 1995), as well as in developing skeletal muscle cells (Williams, 1997). The presence of spatially localized permanent sparking regions has been observed in some of these cells (Williams, 1997). Two-photon calcium uncaging offers the possibility of locally measuring the calcium sensitivity of calcium release in these regions to probe the underlying mechanism of calcium sparking (Shear et al., 1996; Lipp and Niggli, 1998).

To plan an experiment using 2PE of calcium cages, it is useful to predict the amount of calcium release possible upon photolysis of a calcium cage. This requires knowledge of the action cross section of the cage. In this work we report a technique for measuring the absolute two-photon uncaging action cross sections of calcium cages. This technique is potentially applicable to other caged species that can be chelated by a related indicator dye (e.g., Na^+, Mg^{2+}, etc.), as well as to caged fluorescent compounds. The species we have studied are two commercially available calcium cages, DM-nitrophen and NP-EGTA, and a new calcium cage, azid-1 (Adams et al., 1997). The technique used to determine the two-photon action cross sections of calcium cages described in this paper requires a brief pulse train of high-intensity focused laser light within a solution containing caged calcium and a fluorescent calcium indicator dye, such as fluo-3. The high-intensity pulse train releases a fraction of the caged calcium, which is rapidly chelated by the fluorescent indicator dye. The same laser beam that uncages the calcium is attenuated after the photolysis pulse train and is used to generate fluorescence from the indicator dye before it diffuses out of the probe volume. The resultant fluorescence signal has an amplitude that is proportional to the uncaging action cross section and a decay time proportional to the inverse of the diffusion coefficient of the indicator dye.

We find that two of the cages, azid-1 and DM-nitrophen, have measurable two-photon uncaging action cross sections between 700 and 800 nm, with the maximum cross section of azid-1 being ~1.4 GM at 700 nm and the maximum cross section of DM-nitrophen being ~0.013 GM at 730 nm. Using these results, we then calculate the quantities of calcium that can be released in the focal volume with 2PE and explore the temporal behavior of the released calcium concentration distribution as it is influenced by diffusion and buffering.

A summary of the calculations reveals that complete photolysis of some calcium cages is possible with 2PE. Using 700 nm light from a Ti:S laser focused with a 1.3 NA objective into a solution of the cage azid-1, essentially all of the cage within the two-photon focal volume can be photolyzed with a 10 μs pulse train of ~7 mW average power at the sample. DM-nitrophen requires ~74 mW of 730 nm light under similar conditions to achieve essentially complete photolysis. The highly localized distribution of free calcium ions would have a radial dimension of ~0.25 μm and an axial dimension of ~0.86 μm and would dissipate rapidly because of diffusion of free calcium ions and uptake by calcium buffers. In buffer-free cytoplasm, the elevated calcium concentration at the center of the 2PE focal volume can last for ~165 μs full width half-maximum (FWHM), a duration that can be lengthened by increasing the initial spatial extent of release.

MATERIALS AND METHODS

Ca^{2+} uncaging is accomplished using a tunable mode-locked Ti:sapphire (Ti:S) laser (Tsunami; Spectra Physics, Mountain View, CA) that produces ~100 fs pulses at a repetition rate of 81 MHz. The output of the laser is directed through a Pockels cell (model 350-50; Conoptics, Danbury, CT), which serves as a means of rapidly changing the intensity of the laser beam at the sample (see Fig. 1). A 5× beam expander ensures that the beam nearly fills the back aperture of a high-NA microscope objective (1.25 NA 100× oil or 1.2 NA 40× water; Zeiss, Jena, Germany). Samples of the cages NP-EGTA (K_d = 80 nM; Molecular Probes, Eugene, OR), DM-nitrophen (K_d = 5 nM; Calbiochem, San Diego, CA), and azid-1 (K_d = 230 nM; Adams et al., 1997) at 2 mM concentration with 1.04 mM of the calcium indicator dye fluo-3 (K_d = 390; Molecular Probes) and 1.1 mM $CaCl_2$ are sealed in deep-well slides (~500 μm well depth) beneath no. 1.5 coverslips and are positioned with a micrometer driven translation stage so that the two-photon focal volume lies within the well near the coverslip.

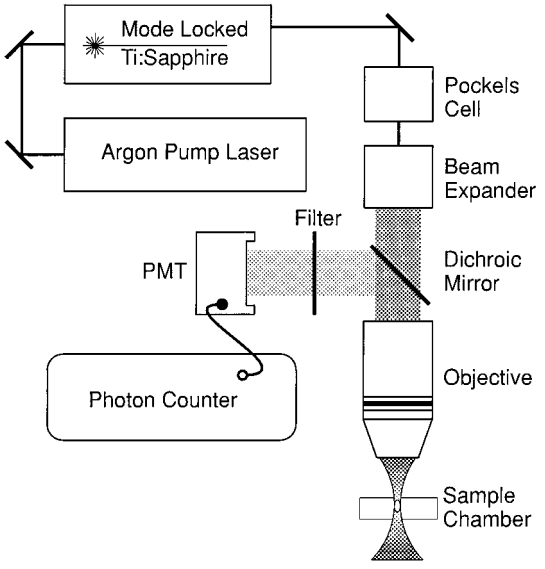

FIGURE 1 Equipment diagram.

The pH of the solution is buffered to 7.3 with 50 mM K-3-(*N*-morpholino)propanesulfonic acid (Sigma Chemical Co., St. Louis, MO), and 98 mM KCl is added to bring the final ionic strength to ~0.15 M. Based upon the relative equilibrium constants of the constituents, we calculate that the concentrations of calcium bound cage/calcium bound indicator dye/free calcium are 0.81 mM/0.29 mM/0.16 μM in the azid-1 solution, 1.1 mM/0.015 mM/5.9 nM in the DM-nitrophen solution, and 0.94 mM/0.16 mM/70 nM in the NP-EGTA solution.

To determine the size of the two-photon focal volume, two-photon fluorescence photobleaching recovery (Brown et al., manuscript submitted) is performed on fluorescent beads with known diffusion coefficients, yielding the e^{-2} focal beam waist of this excitation geometry (the e^{-2} axial dimension of the beam is then calculated from the measured beam waist).

To liberate Ca^{2+} from a cage with high temporal resolution, the Pockels cell throughput is controlled by a voltage signal from a programmable function generator (DS345; Stanford Research Systems, Sunnyvale, CA). At the start of an uncaging sequence, the throughput of the Pockels cell is low, allowing <1 mW to reach the sample. The throughput is then switched to high (to the uncaging intensity) for a brief period (8.5 μs) before being returned to low throughput.

To measure the released Ca^{2+}, a high concentration (~1 mM) of the calcium-sensitive fluorescent dye fluo-3 is present in calcium-free form in the sample solution. The "on" rate constant (k_{on}) for fluo-3 is 7.1×10^8 M^{-1} s^{-1} (Naraghi, 1997). Therefore, a 1 mM solution of fluo-3 binds calcium with a characteristic time of ~1 μs, provided that the quantity released is small enough to avoid significant saturation of the buffer. This rapid uptake time ensures that the liberated calcium will be chelated by fluo-3 well before the ion can diffuse from a 2PE focal volume, even when the highest NA objectives are used. The fluorescence signal of fluo-3 in the solution described above increases by ~180-fold upon binding of calcium, and the resultant change in fluorescence after the photolysis pulse train is monitored using 2PE with the attenuated Ti:S beam. Fluorescence generated by the newly formed calcium bound fluo-3 is collected through the excitation objective and is split off at 90° from the excitation path with a 650-nm long-pass dichroic mirror (650LP; Chroma Technologies, Brattleboro, VT). Two 550-nm bandpass filters (550DF150; Chroma Technologies) are placed immediately in front of a photon-counting photomultiplier tube (PMT) (HC125-02; Hamamatsu, Bridgewater, NJ) to further reject excitation light. One of the cages, azid-1, has an impurity that generates a significant amount of blue fluorescence. This impurity emission interferes with accurate determination of the baseline fluo-3 signal and is therefore attenuated to less than 10% of the fluo-3 signal with an additional 520 nm long-pass colored glass filter. The signal from the PMT is sent to a zero-deadtime photon counter (SR430; Stanford Research Systems), where counts are accumulated in 40.96 μs bins. To reduce shot noise in the data, the pulse-monitoring procedure is repeated 2000–3000 times at a rate (20 Hz) slow enough for diffusion to replenish the two-photon focal volume between repetitions.

The data generated with this equipment are fit to the fluorescence decay curves derived in the following section, which yield the uncaging action cross sections of the cages and the diffusion coefficient of the indicator dye.

MODEL

To derive an action cross section for a calcium cage from a pulsed photolysis experiment, the populations of the ground and excited states of the cage-calcium complex during the photolysis pulse must be calculated. This requires an examination of the photochemistry of the cage. For DM-nitrophen, a photoexcited cage-calcium complex can either relax in the nanosecond time scale without calcium release ($k_0 \approx 10^9$ s^{-1}; Fig. 2) or follow a chemical pathway that results in the release of calcium (McCray et al., 1992). The fraction of photoexcited cages that follow the calcium release pathway is given by q, the quantum yield of uncaging. Those cage-calcium complexes that relax without releasing calcium can be excited again, which provides the possibility of multiple cage excitations during a train of uncaging pulses (McCray et al., 1992).

The photoexcited cages that follow the calcium release pathway first form a nitronic acid intermediate on a nanosecond time scale ($k_a \approx 10^9$ s^{-1}; Fig. 2), then follow a sequence of chemical steps leading to the eventual release of calcium (Ellis-Davies, 1996). The actual rate-limiting step in the production of calcium from photoexcited DM-nitrophen is due to internal bond breakages, whereas for NP-EGTA it is believed to be the final off-rate of the low-affinity photolyzed cage. In both cases, the rate-limiting steps require ~10–20 μs (Ellis-Davies et al., 1996; Escobar et al., 1997), yielding an intrinsic calcium release rate for both types of photoexcited molecules of $k_r \approx 1 \times 10^5$ s^{-1}. Based on the equilibrium constant of photolyzed azid-1 and its presumed on-rate of 7.1×10^8 M^{-1} s^{-1} (equal to that of fluo-3, which has similar calcium-binding properties), this species is predicted to have an intrinsic calcium release rate of $k_r \approx 8.5 \times 10^4$ s^{-1} (Adams et al., 1997). These values of k_r can be confirmed by inspection of

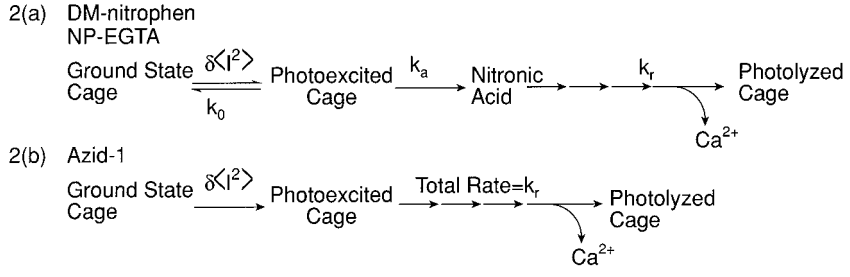

FIGURE 2 Schemes of the internal kinetics of the three cages DM-nitrophen, NP-EGTA, and azid-1. The rate of relaxation of photoexcited cage via the pathway in system *a* that does not release calcium is $k_0 \approx 1 \times 10^9$ s^{-1} (McCray et al., 1992). The rate of production of the nitronic acid intermediate is $k_a \approx 2 \times 10^8$ s^{-1} and is calculated from k_0 using the quantum yield of the cage. The rate-limiting rate of calcium release from a photoexcited cage as dictated by internal conformational shifts of an excited cage is $k_r \approx 8 \times 10^4$ s^{-1} for system *a* (Ellis-Davies et al., 1996) and $k_r \approx 8.5 \times 10^4$ s^{-1} for system *b*, based upon the equilibrium constant of azid-1 and its presumed on-rate of 7.1×10^8 M^{-1} s^{-1} (Adams et al., 1997).

the change of indicator dye fluorescence signal, $\Delta F/F_0$, as shown in Fig. 3. As will be explained, this normalized fluorescence signal provides a measure of the calcium released in the focal volume by a photolysis pulse train. A rate-limiting uncaging step that is comparable to or longer than the time bins used to record this fluorescence signal would result in a detectable delay in achieving the peak fluorescence after the termination of the uncaging pulse. No such rise time is observed for any of the cages in data taken with 41 μs time bins (see Fig. 3), suggesting that the rate-limiting step for the three cages is indeed faster than the maximum temporal resolution of the measurements.

These factors suggest that a simplified kinetic diagram as in Fig. 2 *a* is appropriate for DM-nitrophen and NP-EGTA. The overall uncaging quantum yield of the third cage in this paper, azid-1, is ~1.0 (Adams et al., 1997); thus we can neglect cage recycling during the pulse and assume that it follows the simplified kinetic diagram, as shown in Fig. 2 *b*.

The rapid rate constants k_a of the first step in the reaction pathway of DM-nitrophen and NP-EGTA suggests that diffusional quenching of these species can be neglected, because the estimated diffusional interaction time of molecules of this size at 2 mM concentration is ~200 ns, whereas the excited-state lifetime is $1/k_a \approx 1$–10 ns. Azid-1 has a similar ~1 ns excited-state lifetime (Adams et al., 1997), allowing neglect of diffusional quenching of this species. The excited-state lifetime of fluo-3 is <3 ns (Draaijer et al., 1995), which is much shorter than the predicted diffusional interaction time of ~200 ns, and diffusional quenching is neglected for this species as well.

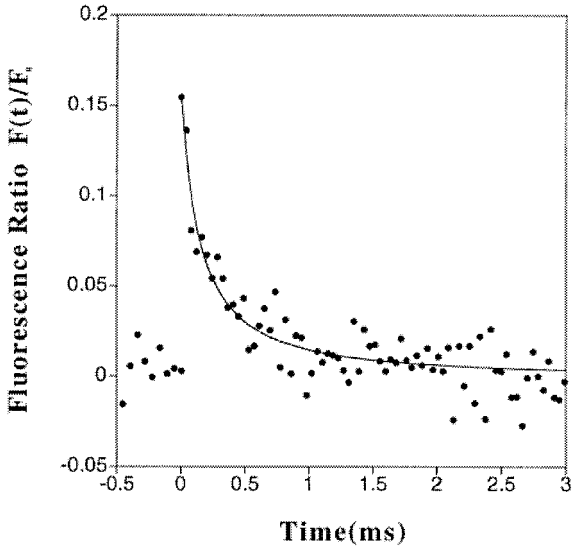

FIGURE 3 Normalized two-photon uncaging signal of azid-1 at 700 nm. The bright pulse train of laser light occurs at $t = 0$, generating new calcium-bound fluo-3, which produces an increase ΔF in fluorescence signal relative to the initial equilibrium fluorescence F_0. This fluorescence decays away as the new calcium-bound fluo-3 diffuses out of the two-photon focal volume generated by the 1.25 NA objective. The solid line is a fit to the data using Eq. 8. The two fitting parameters are the diffusion coefficient of the calcium-bound fluo-3 complex ($D \approx 0.8 \times 10^{-6}$ cm^2 s^{-1}) and the uncaging action cross section of azid-1 ($\delta_u = 1.4$ GM).

Once we have defined a kinetic model for each cage, we can solve the differential equations characterizing the populations of the various states after an uncaging pulse of duration Δt and average squared intensity $\langle I_u^2(r, z)\rangle$, where r and z are the radial and axial distances from the center of the two-photon focal volume. In these experiments, the duration of uncaging pulse trains is much larger than the characteristic relaxation time of the processes that do not release calcium ($k_0 \approx 1$ ns; see Fig. 2), allowing multiple excitations of cages that follow this path. For DM-nitrophen and NP-EGTA we therefore take the limit that the uncaging pulse train is much longer than the excited-state lifetime of the cage, $\Delta t \gg 1/(k_0 + k_a)$. Furthermore, in the limit that k_0, $k_a \gg \frac{1}{2}\delta_u\langle I_u^2(r, z)\rangle$ (which is applicable to these cages under normal illumination conditions), we find that the concentration of calcium released under kinetic scheme 2 *a* in the limit of no saturation is

$$\Delta[Ca^{2+}(r, z)] = (1 - e^{-(1/2)\delta_u\langle I_u^2(r,z)\rangle\Delta t})[CCa^{2+}]_0 \qquad (2)$$

where $\Delta[Ca^{2+}(r, z)]$ is the amount of free calcium generated by photolysis, $[CCa^{2+}]_0$ is the equilibrium concentration of calcium-loaded cage, and $\delta_u \equiv q\delta$ is the uncaging action cross section. The quantum yield of the kinetic process in Fig. 2 *a* is $q = k_a/(k_a + k_0)$. It is a straightforward calculation to determine that Eq. 2 also applies to kinetic scheme 2 *b*, which governs cages with a quantum yield of ~1.0, such as azid-1.

Equation 2 assumes that diffusion of cage molecules is negligible during the excitation pulse train. The characteristic diffusional escape time for cage molecules out of the focal volume will be similar to the diffusional escape time of fluo-3, which is ~0.3 ms for the focal volume produced by a 1.25 NA microscope objective illuminated at 700 nm (see Fig. 3); therefore, to satisfy our assumption, the excitation pulse train duration Δt must be significantly less than this value.

The calcium that is released in these experiments enters an environment with ~1 mM of calcium-free fluo-3. At this concentration fluo-3 binds calcium in a characteristic time of ~1 μs, much shorter than the characteristic diffusion time needed for the calcium to diffuse from the focal volume of the objective. As a result, essentially all of the released calcium can be chelated before it can diffuse out of the focal volume. Not all of the chelated calcium is necessarily chelated by fluo-3, however. With a presumed k_{on} of 7.1×10^8 M^{-1} s^{-1} and a concentration of 1.19 mM, calcium-free azid-1 has a characteristic uptake time of 1.2 μs, which is sufficiently rapid to compete with fluo-3 for liberated calcium ions. With a k_{on} of 3.5×10^7 M^{-1}s^{-1} (T. Xu et al., 1997) and a concentration of 0.9 mM, calcium-free DM-nitrophen has a characteristic uptake time of 32 μs, whereas calcium-free NPEGTA, with a k_{on} of 1.7×10^7 M^{-1}s^{-1} (Ellis-Davies et al., 1996) and a concentration of 1.06 mM, has a characteristic uptake time of 55 μs. Neither

of these calcium-free species competes significantly with calcium-free fluo-3 for the liberated calcium ions. Consequently, for the NPEGTA and DM-nitrophen samples it is assumed that essentially all of the liberated calcium is chelated by calcium-free fluo-3, whereas for the azid-1 sample the relative uptake by the two buffers is estimated and is used as a correction factor in the determination of the action cross section.

With these assumptions, the spatial distribution of new calcium-bound fluo-3 $\sim$10 μs ($1/k_r$) after the uncaging pulse is

$$\Delta[\mathrm{FCa}^{2+}(r, z; t = 0)] = [\mathrm{CCa}^{2+}]_0(1 - e^{-(1/2)\delta\langle I_u^2(r,\, z)\rangle\Delta t}) \qquad (3)$$

where $\Delta[\mathrm{FCa}^{2+}(r, z; t = 0)]$ is the local concentration of new calcium-loaded fluo-3. This newly formed calcium-bound fluo-3 is added to the existing background (baseline) distribution of calcium-bound fluo-3 (as determined by the relative equilibrium constants of fluo-3 and cage). The off-rate of fluo-3, calculated from its K_d and on-rate, is $\sim$277 s^{-1}, indicating that this newly formed calcium-bound fluo-3 will release calcium on time scales of $\sim$3.6 ms. This is much slower than the $\sim$0.3 ms diffusional escape time of this species from the two-photon focal volume (see Fig. 3), so fluo-3 can be assumed not to achieve equilibrium with the newly generated calcium, and to act only as a calcium sink, not as a calcium source. The fluorescence signal the new calcium bound fluo-3 produces is then given by

$$\Delta F(t) = E\int \Delta[\mathrm{FCa}^{2+}(r, z, t)]\tfrac{1}{2}\delta_f\langle I_m^2(r, z)\rangle \mathrm{d}v \qquad (4)$$

where E is the collection efficiency of the detection system, δ_f is the fluorescence action cross section of calcium-bound fluo-3, and $\langle I_m^2(r, z)\rangle$ is the time average of the square of the local monitoring intensity.

The time dependence of this fluorescence signal over the period of calcium-bound fluo-3 efflux from the probe volume can be calculated once the spatial distribution of the new calcium-bound fluo-3, $\Delta[\mathrm{FCa}^{2+}(r, z, t)]$, is known. This distribution is determined by applying the diffusion equation to the initial distribution given by Eq. 2. The diffusion calculation yields an analytical solution only for the ellipsoidal Gaussian approximation to the diffraction-limited focus, where the illumination pattern of an overfilled objective is approximated by

$$I_u(r, z) = I_u(0,0)e^{-(2r^2/w_r^2 + 2z^2/w_z^2)} \qquad (5)$$

where w_r is the radial e^{-2} beam waist, w_z is the axial e^{-2} distance, and $I_u(0,0)$ is the excitation intensity of the uncaging beam at the center of the focal spot. Use of this illumination pattern yields a final result for the time-dependent fluorescence signal of the newly generated calcium bound fluo-3:

$$\Delta F(\tau) = [\mathrm{CCa}^{2+}]_0 E\,\frac{\delta_f}{2}\langle I_m^2\rangle\,\frac{w_r^3}{8R^{1/2}}\,\pi^{3/2} \times\left(-\sum_{n=1}^{\infty}\frac{\left(-\frac{\delta_u}{2}\langle I_u^2\rangle\Delta t\right)^n}{n!(1 + n(1 + 2\tau))(1 + n(1 + 2R\tau))^{1/2}}\right) \qquad (6)$$

where R is the square of the ratio of the two e^{-2} beam waists and τ is a dimensionless "time" equal to $8D_f t w_r^{-2}$ (D_f is the diffusion coefficient of fluo-3).

These experiments take place in the low uncaging limit, $\frac{1}{2}\delta_u\langle I_u^2\rangle\Delta t < 1$, to prevent depletion of the calcium-free fluo-3 in the focal spot. Only the first term in the series contributes significantly in this regime, and the uncaging yield scales as intensity squared. Taking this limit, the fluorescence of the newly generated calcium is

$$\Delta F(\tau) = \frac{F_0\delta_u\langle I_u^2\rangle\Delta t}{4\sqrt{2}(1 + \tau)(1 + R\tau)^{1/2}}\,\frac{[\mathrm{CCa}^{2+}]_0}{[\mathrm{FCa}^{2+}]_0} \qquad (7)$$

where F_0 is the average fluorescence of the equilibrium concentration of calcium-bound fluo-3, $[\mathrm{FCa}^{2+}]_0$.

The time average of the intensity squared at the sample is difficult to measure directly; an alternative approach is to use the steady-state fluorescence of the calcium-bound fluo-3 in solution as an internal standard. When rewriting $\langle I_u^2\rangle$ in terms of the fluorescence F_0 of the calcium-bound fluo-3 already in solution, we find

$$\Delta F(\tau) = \left(\frac{2}{\pi}\right)^{3/2}\frac{\delta_u\gamma^2F_o^2R^{1/2}\Delta t}{\delta_f E w_r^3(1 + \tau)(1 + R\tau)^{1/2}}\,\frac{[\mathrm{CCa}^{2+}]_0}{[\mathrm{FCa}^{2+}]_0^2} \qquad (8)$$

where γ is the ratio of the average powers of the uncaging and monitoring beams and E is the efficiency of the detection system.

In the azid-1 and NPEGTA samples, the high equilibrium concentration of calcium-bound fluo-3 combined with the extremely low fluorescence signal of calcium-free fluo-3 means that the contribution of the calcium-free species to the total equilibrium fluorescence signal is small (<3%) and essentially constant and can be neglected for the purposes of this measurement. In the DM-nitrophen sample, however, the concentration of calcium-free fluo-3 is significantly larger (68×) than that of calcium-bound fluo-3, and this species contributes $\sim$27% of the total equilibrium fluorescence signal (based upon the equilibrium concentrations of the two species and their relative fluorescence yields of 180:1). The nonequilibrium transient fluorescence increase, $\Delta F(t)$, generated by a photolysis pulse train in the DM-nitrophen sample is dominated by the change in the concentration of the calcium-bound fluo-3, and the variation in the fluorescence signal due to the calcium-free species is a negligible ($\sim$1/180) portion of the overall transient signal.

Consequently, the contribution of the calcium-free species to the fluorescent signal is treated as a constant correction factor for this sample.

The uncaging fluorescence decay curves (such as the one shown in Fig. 3) can be fit to Eq. 8 to determine the ratio of the two-photon action cross sections of the various cages to the two-photon action cross section of calcium-bound fluo-3 at the same wavelength. The absolute action cross sections of the cages are then determined using previously measured values for the absolute cross section of fluo-3.

RESULTS OF THE ACTION CROSS SECTION MEASUREMENTS

The uncaging pulse train protocol was first followed with solutions containing only fluo-3 and calcium to determine the range of uncaging powers that does not significantly bleach fluo-3. All subsequent uncaging experiments were performed at uncaging powers that yielded no measurable fluo-3 bleaching (i.e., $\leq$1% bleaching signal). The exact equilibrium concentration of calcium-bound fluo-3 was determined from the equilibrium fluorescence signal of each sample and comparison to calcium-saturated and calcium-free fluo-3 standards. The concentration of calcium-bound cage was then found by assuming that the calcium not bound to fluo-3 was bound to cage, neglecting the extremely small amount of calcium expected to remain free.

A typical fluorescence curve generated by an uncaging pulse train photolyzing azid-1, with the corresponding fit to Eq. 8, is shown in Fig. 3. Equations 3 and 7 applied to the $t = 0$ point on the curve reveal that the concentration of calcium-loaded fluo-3 at the center of the two-photon focal volume is ~120 μM. The total concentration of calcium liberated at the center of the focal volume (and bound to the buffers present at high concentrations) is therefore at least 120 μM and is in fact closer to ~300 μM once the competition of calcium-free azid-1 with fluo-3 has been factored in (see below). This means that even at these gentle doses, which do not significantly bleach fluo-3, ~40% of the cage at the center of the focal volume has been photolyzed.

The amplitude of the transient increase in fluo-3 fluorescence as a function of the photolysis power is shown in Fig. 4. At low uncaging powers, the increase in fluo-3 fluorescence immediately after the uncaging pulse scales approximately with power squared, as expected for a two-photon photolysis process where the fluorescent indicator dye is not being significantly depleted by the released calcium.

The two-photon uncaging action cross sections of azid-1 and DM-nitrophen are shown in Fig. 5 for a range of excitation wavelengths between 700 and 800 nm. Azid-1 has a maximum action cross section of ~1.4 GM at 700 nm, and DM-nitrophen has a maximum action cross section of ~0.013 GM at 730 nm. The uncaging signal from NP-EGTA is too weak at any of the wavelengths studied to detect above the background noise.

The action cross section for azid-1 must be calculated while taking into account the presence of significant amounts of unphotolyzed calcium-free azid-1 that compete with fluo-3 for liberated calcium. In these nonequilibrium

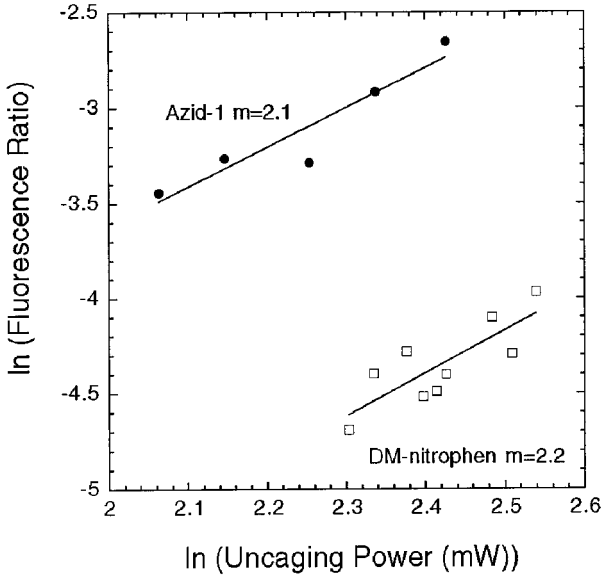

FIGURE 4 Evidence for the two-photon nature of the uncaging of DM-nitrophen and azid-1 between 700 and 800 nm. The ratio of the increase in fluorescence immediately after the photolysis pulse ΔF ($\tau = 0$) to the equilibrium fluorescence F_0 is plotted against the average power of the uncaging pulse train, yielding the expected power squared dependence at low uncaging yields. Azid-1 was photolyzed with 8.5 μs trains of 100 fs pulses at 80 MHz and 760 nm, and DM-nitrophen was photolyzed with equivalent pulse trains at 730 nm.

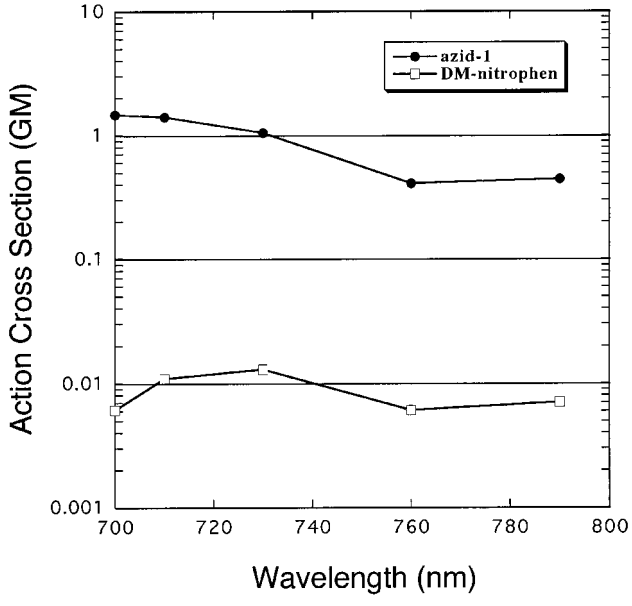

FIGURE 5 The two-photon uncaging action cross sections of azid-1 and DM-nitrophen between 700 and 800 nm expressed in GM, where 1 GM = 10^{-50} cm^4 s photon^{-1}. The values of the measured action cross sections are certain to within a factor of 2. NP-EGTA did not produce enough calcium for a reproducible uncaging signal to be detected above background noise at any of the wavelengths studied.

conditions the fraction of calcium chelated by calcium-free fluo-3 can be closely approximated by the effective on-rate of this species (given by the concentration times the rate constant k_{on}) divided by the sum of the effective on-rates of calcium free fluo-3 and azid-1. In these experiments, calcium-free azid-1 was estimated to be present at a concentration of 1.2 mM, with a k_{on} approximately equal to that of fluo-3. Given that the concentration of free fluo-3 was 0.75 mM, only ~39% of the liberated calcium was chelated by fluo-3 after it was released from photolyzed azid-1, with the rest going to calcium-free azid-1. The reported action cross section value reflects a correction for incomplete chelation by fluo-3.

The action cross section for DM-nitrophen must be calculated while taking into account the contribution of calcium-free fluo-3 to the equilibrium fluorescence signal. The relative signal of calcium-bound fluo-3 to calcium-free fluo-3 is 180:1 in this chemical environment, and the relative concentration of the two species is 0.015. This means that the equilibrium fluorescence signal from calcium-loaded fluo-3, F_0, is only 73% of the total equilibrium fluorescence signal. The reported action cross section for DM-nitrophen reflects a correction for the equilibrium signal of calcium-free fluo-3.

The relative two-photon action cross sections of these three cages are consistent with their one-photon absorption properties. The product of the extinction coefficient times the quantum efficiency of azid-1 is 33,000 M^{-1} cm^{-1} and peaks at ~340 nm (Adams, et al., 1997), whereas the same product is only 780 M^{-1} cm^{-1} for DM-nitrophen, and this species has a peak absorptivity at ~360 nm (Kaplan and Ellis-Davies, 1988). The absorption peak of NP-EGTA is at ~260 nm, and the peak extinction coefficient times the quantum efficiency is 1270 M^{-1} cm^{-1} and drops to 224 M^{-1} cm^{-1} at 347 nm (Ellis-Davies and Kaplan, 1994). Although the two-photon cross section of a chromophore does not always peak at twice the wavelength of the one-photon cross section peak, this is often a first assumption for qualitatively predicting the location of the two-photon peak (Xu and Webb, 1997). We would therefore expect the two-photon action cross section of azid-1 to be much higher than the other two cages studied and to peak at ~680 nm, whereas DM-nitrophen should be considerably less excitable than azid-1 and should peak at ~720 nm. This is in excellent agreement with the data shown in Fig. 5. From the one-photon data, we would expect the two-photon action cross section of NP-EGTA to be peaked at ~520 nm, well outside the accessible range of the Ti:sapphire laser, and to have an extremely low action cross section at ~690 nm, so it is not surprising that this cage did not have a measurable signal between 700 and 800 nm.

The lack of an uncaging signal generated by photolysis of NP-EGTA with this technique may also be due to its equilibrium constant. The curve described by Eq. 7 is a fluorescence signal $\Delta F(\tau)$ superimposed upon a baseline fluorescence F_0 that arises from the equilibrium loading of fluo-3. Within the range of uncaging intensities that do not cause substantial bleaching of fluo-3, the transient signals we observed for all cages were significantly less intense than the steady-state fluorescence F_0. As a result, the noise in the total fluorescence amplitude is dominated by the shot noise from the baseline fluorescence F_0. The desired signal is the change in fluorescence due to newly generated calcium-bound fluo-3, $\Delta F(\tau)$; therefore assuming that F_0 is shot noise limited, the signal-to-noise ratio of this technique is

$$\frac{S}{N} \propto \frac{\Delta[FCa^{2+}]}{[FCa^{2+}]_0^{1/2}} \propto \delta_{uc} \frac{[CCa^{2+}]_0}{([FCa^{2+}]_0)^{1/2}} \quad (9)$$

Clearly, S/N is a function of δ_{uc} but also has important contributions from the equilibrium loading of cage and indicator dye. Hence when all other factors are equal, the overall signal-to-noise ratio is better when cages are used that have low K_d values. DM-nitrophen has the lowest dissociation constant of the three tested here, with $K_d \approx 5$ nM in the absence of competing Mg^{2+}. The K_d of NP-EGTA is 80 nM, more than 10 times greater than that of DM-nitrophen. This factor reduces the signal-to-noise ratio by more than threefold compared to DM-nitrophen. Thus the absence of measurable NP-EGTA uncaging in these studies can be attributed to the high equilibrium constant of this species as well as to a small two-photon uncaging action cross section.

The primary sources of error in the reported action cross section values are the uncertainty in the e^{-2} radii and determination of the detection efficiency E. Neither of these factors affects the relative values of the two-photon action cross section of DM-nitrophen or azid-1 at different wavelengths, but they lead us to conclude that the absolute values of the action cross sections are correct only to within a factor of 2.

ANALYSIS OF THE YIELD AND DYNAMICS OF LIBERATED CALCIUM

Total calcium yield

To directly measure the amount of calcium liberated during a pulse train, significant bleaching of the indicator dye should be avoided. In addition, binding of liberated calcium to dye should not substantially deplete the concentration of calcium-free dye. To reach such a useful regime, these experiments have been limited to low uncaging yields in solutions containing a high concentration of fluo-3. Biological applications may require caged calcium to be used with no fluorescent indicator dye present or to be more fully photolyzed than in these experiments, causing substantial bleaching of the indicator dye. Such conditions would preclude direct measurement of the amount of calcium released. However, once the action cross section of a calcium cage is known, it is possible to calculate the amount of calcium freed with a given excitation pulse train. Assuming that the total solution volume is much larger than the two-photon focal volume, Eq. 2 can be integrated over all space

to yield N_{Ca}, the net number of calcium ions liberated by a diffraction-limited uncaging pulse train of duration Δt:

$$N_{Ca} = -N[CCa^{2+}]_0 \frac{\pi^{3/2} w_r^2 w_z}{8} \sum_{n=1}^{\infty} \frac{(-1/2\delta_u \langle I_u^2 \rangle \Delta t)^n}{n! n^{3/2}} \quad (10)$$

where N is Avogadro's number. This expression contains terms proportional to the equilibrium number of cage-calcium complexes in the two-photon focal volume, as well as terms that describe the fractional release of these ions. Equation 10 can be simplified by dividing the entire equation by the equilibrium number of cage-calcium complexes in the focal volume, thereby expressing the uncaging production as a fractional yield. This simplification requires the choice of an appropriate definition of the two-photon focal volume, V. A definition of V that arises from analysis of multiphoton fluorescence correlation spectroscopy (Mertz et al., 1995) is

$$V \equiv \frac{(\int I_u^2(r, z) dv)^2}{\int I_u^4(r, z) dv} \quad (11)$$

With this choice for the 2PE focal volume we calculate the "uncaging ratio" R_u, defined as the number of calcium ions generated by a photolysis pulse illuminating a diffraction-limited volume (Eq. 10) divided by the number of cage-calcium complexes available to be photolyzed in the two-photon focal volume V:

$$R_u = -\frac{\sqrt{2}}{4} \sum_{n=1}^{\infty} \frac{(-\alpha)^n}{n! n^{3/2}} \quad (12)$$

In this expression $\alpha \equiv \frac{1}{2}\delta_u \langle I_u^2 \rangle \Delta t$, the "central uncaging dose," denotes the average number of uncaging events per molecule at the center of the two-photon volume in the low-intensity limit. Note the nonintuitive result that the uncaging ratio R_u does not asymptotically approach one. This is because the chosen mathematical representation of the two-photon volume V is defined in the low-excitation intensity limit, without ground-state depletion of the fluorophore undergoing 2PE (Mertz et al., 1995). At high enough central uncaging doses ($\alpha > 6$), significant numbers of cage-calcium complexes that lie in the lower intensity periphery of the illumination profile can be photolyzed; Eq. 11 underestimates the effective volume of release. Consequently, Eq. 12 predicts that the uncaging ratio grows without bound as the central uncaging dose α approaches infinity.

For central uncaging doses between zero and 35, Eq. 12 can be approximated by the following expression, which is plotted in Fig. 6.

$$R_u \cong 2.54 - 1.967e^{-0.0543\alpha} - 0.572e^{-0.405\alpha} \quad (13)$$

Equation 13 can be used to predict the excitation dose α required to release a given amount of caged calcium. To photolyze a total number of cage-calcium complexes equal to the number contained in the two-photon volume V, i.e., an uncaging ratio R_u of 1, the central uncaging dose α needs to be ~6 or more.

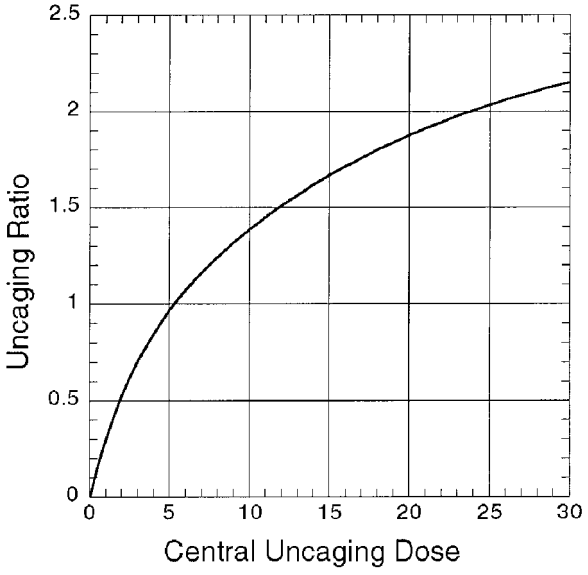

FIGURE 6 The calculated uncaging ratio R_u as a function of the central uncaging dose $\alpha = \frac{1}{2}\delta_u \langle I_u^2 \rangle \Delta t$. The uncaging ratio is defined as the total number of calcium ions liberated divided by the total equilibrium number of cage-calcium complexes available to be photolyzed within the two-photon focal volume and is calculated using Eq. 13.

Azid-1 requires 700 nm light of 7 mW average power overfilling the aperture of a 1.3 NA objective in a 10 μs train of 100 fs pulses at 80 MHz to achieve an uncaging ratio of 1. DM-nitrophen needs 74 mW at the sample to achieve a similar uncaging ratio at its peak wavelength of 730 nm. When uncaging periods are increased to 40 μs, this intensity requirement decreases by approximately twofold.

Temporal behavior of released calcium

The temporal behavior of the calcium concentration distribution generated by a 2PE photolysis pulse train will be an important factor in the design of many uncaging experiments. This behavior will be dominated by the competition for liberated calcium between various extrinsic buffers, intrinsic buffers, and diffusion out of the two-photon focal volume. The complex nature of this interaction between buffering and diffusion over the subfemtoliter spatial scales of multiphoton uncaging makes exact calculation of the resultant calcium concentration distributions problematic. To gain a physical understanding of the dynamics of the calcium concentration after a photolysis pulse without attempting to numerically solve the relevant differential equations, we will restrict our attention to the temporal behavior of the calcium concentration at the center of the two-photon focal volume and model this behavior using a few approximations that greatly simplify the problem.

We can represent the diffusion of free calcium ions out of the two-photon focal volume as a simple first-order process with an effective rate k_{df} that scales as the inverse of the

average dwell time, which for objectives having NAs between 0.6 and 1.3 we will approximate as $k_{df} \cong 1.2D_{Ca}/w_r^2$, where D_{Ca} is the true diffusion coefficient of free calcium ions. This has been measured as $D_{Ca} = 2.2 \times 10^{-6}$ cm^2 s^{-1} for calcium ions in cytoplasm (Albrittion et al., 1992) and $D_{Ca} = 8 \times 10^{-6}$ cm^2 s^{-1} for calcium ions in water (Robinson and Stokes, 1959).

If we restrict our photolysis production so that the peak liberated calcium concentrations are significantly smaller than the local concentrations of free calcium buffers, we can assign effective uptake rates for intrinsic and extrinsic calcium buffering (k_i and k_x, respectively), which are the products of the on-rate constants of the buffers (with units of M^{-1} s^{-1}) and the concentrations of free buffer. For simplicity, we are assuming that calcium buffers diffuse out of the two-photon focal volume at a much faster rate than their off-rate and act purely as calcium sinks, not as calcium sources. The predicted off-rate of fluo-3, based upon its K_d and on-rate constant, is ~277 s^{-1}, yielding a characteristic time for calcium release of ~3.6 ms. The diffusional escape time out of a 1.33 NA focal volume in water, based upon inspection of Figure 3, is ~0.3 ms, and this is probably a valid assumption for this buffer. This is also likely to be a valid assumption for various mobile cytoplasmic buffers such as calbindin, which has k_{off} ~50 s^{-1} (Forsen et al., 1988) and an expected escape rate from a 700 nm, 1.33 NA focal volume of ~370 s^{-1}, based upon its estimated cytoplasmic diffusion coefficient of ~1.5 × 10^{-7} cm^2 s^{-1} (Klingauf and Neher, 1997). For poorly mobile buffers or buffers with high off-rates, however, this assumption may not be valid.

We can now assign a single effective rate k_e for dissipation of a calcium ion from the two-photon focal volume to account for all of the processes of calcium removal. This effective rate is the sum of the effective rates for diffusion of free calcium ions out of the focal volume (k_{df}), chelation by intrinsic buffer (k_i), and chelation by extrinsic buffer (k_x). We will initially consider photolysis of the cage with the highest cross section for 2PE, azid-1. This species has a quantum efficiency of ~1.0, and we are therefore able to neglect relaxation pathways for photoexcited cages that do not release calcium, simplifying our calculation.

Using these approximations, we can now define an extremely simple relationship between the concentrations of the various species that are relevant when a photolysis pulse train acts upon a solution of caged calcium:

$$[CCa^{2+}(0,0;t)] \xrightarrow{(1/2)\delta_u\langle I_u^2\rangle} [C^*Ca^{2+}(0,0;t)] \qquad (14)$$

$$\xrightarrow{k_r} \Delta[Ca^{2+}(0,0;t)] \xrightarrow{k_e} \text{Escape}$$

where $[CCa^{2+}(0,0;t)]$ is the concentration of ground-state cage-calcium complexes at the center of the two-photon focal volume, $[C^*Ca^{2+}(0,0;t)]$ is the concentration of photoexcited cage calcium complexes at the center of the focal volume, $\Delta[Ca^{2+}(0,0;t)]$ is the concentration of liberated calcium ions at the center of the two photon focal volume, and Escape represents the escape of liberated calcium ions from the system either through uptake by local buffers or by diffusion out of the focal volume.

To generate highly localized calcium distributions of high concentration, rapid uncaging pulses ($\Delta t \ll 1/k_e$) of high uncaging rate ($\frac{1}{2}\delta_u\langle I_u^2\rangle \gg k_r, k_e$) will be used. Under these conditions, the differential equations represented diagrammatically by Eq. 14 can be solved to yield the increase in free calcium concentration at the center of the two-photon focal volume after an uncaging pulse train:

$$\Delta[Ca^{2+}(0,0;t)] = \frac{k_r}{(k_r - k_e)}(e^{-k_e t} - e^{-k_r t})[CCa^{2+}]_0 \qquad (15)$$

Equation 15 can be used to predict the temporal behavior of the peak calcium concentration under a variety of experimental conditions. This temporal behavior is also valid for a cage of nonunity quantum efficiency such as DM-nitrophen, although in that case $[CCa^{2+}]_0$ should be replaced by the local concentration of cage that is successfully photolyzed by the excitation pulse, given by Eq. 2. For physiological doses this will not generally be equal to $[CCa^{2+}]_0$ because of the low cross section of DM-nitrophen.

To explore the effects that varying the spatial resolution of calcium release has on the duration of calcium elevations generated with a two-photon photolysis pulse, we apply Eq. 15 to 2PE of DM-nitrophen in cytoplasm with no calcium buffering. The combined effective escape rate k_e only has contributions from free calcium diffusion out of the two-photon focal volume. Calculations for 0.5- and 1.3-NA objectives overfilled with 700-nm light are shown in Fig. 7. We see that the calcium elevations generated with the superior spatial resolution of high NA optics can last up to ~165 μs FWHM. Both the amplitude and the duration of the free calcium pulse decrease with increasing NA because of the faster diffusional escape time from the smaller focal volume of the higher NA objective. Note, however, that producing similar central uncaging doses α while lowering the NA of the objective requires a significant increase in input power.

To explore the effects that calcium buffers have on the duration of calcium elevations generated with two-photon photolysis pulses, we will apply Eq. 15 to two hypothetical experiments, one using the cage DM-nitrophen in the presence of a model intrinsic cellular buffer and one using the cage azid-1 in the presence of a model intrinsic cellular buffer and an extrinsic calcium indicator dye. A cell with an equilibrium free calcium concentration of 100 nM that has been loaded with 1 mM DM-nitrophen with a Mg^{2+}-free patch pipette should have 950 μM calcium-loaded cage (based upon its magnesium-free K_d). A 2 μs photolysis pulse train of 7 mW of 730 nm light will produce an uncaging dose of $\alpha \approx 0.01$ and an uncaging ratio of $R \approx 0.005$. This means that only ~0.5% of the cage molecules in the two-photon focal volume will be photolyzed. The concentration of photoexcited cage-calcium complexes at the

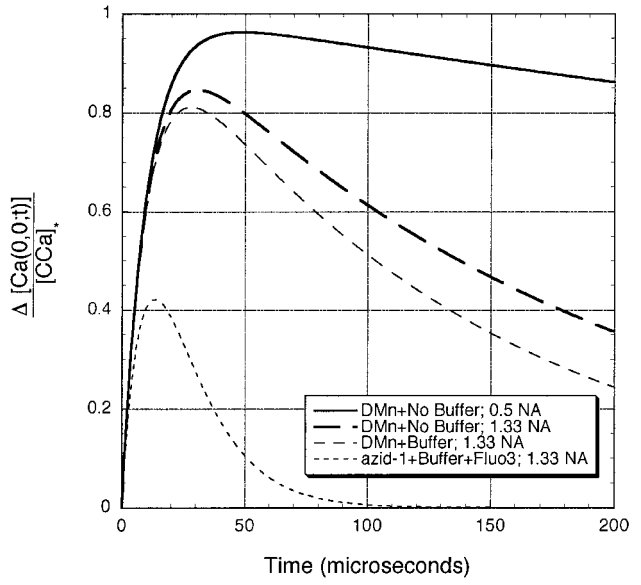

FIGURE 7 The estimated free calcium concentration at the center of the two-photon focal volume, as expressed by Eq. 15. The concentration is given as a ratio of the local liberated calcium concentration to the equilibrium concentration of cage-calcium complexes before the uncaging pulse train in the case of azid-1, or to the concentration of photoexcited cage-calcium complexes generated by the uncaging pulse train in the case of DM-nitrophen. Compare heavy lines to observe the effect of varying the NA of the objective, and dashed lines for the addition of varying amounts of calcium buffers. "Buffer" in the legend signifies the presence of 100 μM calcium-free mobile buffer with an on-rate and diffusion coefficient equal to those of calbindin, and "Fluo3" signifies the presence of 80 μM calcium-free fluo-3.

center of the focal volume should be $0.011 * 950\ \mu M \approx 11\ \mu M$ (see Eq. 2), and these complexes should release their calcium ions with a characteristic release rate of $k_r \approx 1 \times 10^5\ s^{-1}$. If we assume that the total calcium buffering effect is equivalent to that exerted by 100 μM of a mobile calcium buffer (Klingauf and Neher, 1997), with an on-rate in this magnesium-free, high ionic strength environment equal to that of calbindin ($k_{on} \approx 2 \times 10^7\ M^{-1}\ s^{-1}$; Martin et al., 1990), then $k_i = 2 \times 10^3\ s^{-1}$; the predicted behavior of the free calcium is shown in Fig. 7.

A cell with an equilibrium calcium concentration of 100 nM that has been loaded with 100 μM fluo-3 and 10 μM azid-1 should have 3.03 μM calcium-loaded azid-1 and 80 μM calcium-free fluo-3 (based upon their K_d's). Equation 12 predicts that a 2 μs, 15 mW pulse train of 730 nm light overfilling a 1.33 NA lens will achieve an uncaging dose of $\alpha \approx 6$ and therefore an uncaging ratio of 1. This means that essentially all of the cage molecules in the two-photon focal volume will be photolyzed. Equation 2 predicts that the concentration of photoexcited cage-calcium molecules at the center of the focal volume will be $0.998 * 3.03\ \mu M \approx 3\ \mu M$. We again expect that these photoexcited molecules will release their calcium ions with an intrinsic release time of $1/k_r \approx 12\ \mu s$, into a cell with 80 μM fluo-3 and cellular buffer, which we will again model with a mobile buffer with a concentration of 100 μM and an on-rate of $2 \times 10^7\ M^{-1}\ s^{-1}$. The contribution to the calcium uptake rate by the ~10 μM photolyzed azid-1 at the center of the focal volume will be negligible compared to the contributions due to extrinsic and intrinsic buffers, and the combined rate for calcium loss from the center of the two-photon focal volume will be $k_0 = (80\ \mu M)(7.1 \times 10^8\ M^{-1}\ s^{-1}) + (100\ \mu M)(2 \times 10^7\ M^{-1}\ s^{-1}) + (5.45 \times 10^3\ s^{-1}) = 6.4 \times 10^4\ s^{-1}$. With these values for k_r and k_0, Eq. 15 gives an estimate of the temporal behavior of the concentration of free calcium at the center of the two-photon focal volume shown in Fig. 7, suggesting that the free calcium will rise to a peak of $0.42 * [CCa^{2+}]_0 \approx 1.3\ \mu M$ and will last for ~33 μs (FWHM).

These two examples demonstrates the familiar trade-off between fluorescence signal and biological effect; when a calcium indicator dye (i.e., an extrinsic calcium buffer) is used to image the cellular behavior induced by uncaging calcium, the concentration of free calcium available to initiate this behavior is reduced.

If the total concentration of the cage azid-1 is high enough that the uptake rate of photolyzed cage becomes a significant fraction of the uptake rate due to other buffers, the contribution of photolyzed cage to k_e must be considered. In this case, application of Eq. 15 becomes problematic because this species is expected to have a fast off-rate compared to its diffusional escape time, thereby violating our assumption that the calcium buffers act only as calcium sinks, not sources.

Steady-state MPE calcium release

The simple model given by Eq. 14 can also predict the steady-state calcium concentration at the center of the two-photon focal volume, $[Ca^{2+}]_{ss}$, maintained by continuous two-photon excitation of a calcium cage in the absence of calcium buffers:

$$[Ca^{2+}]_{ss} \cong \frac{\frac{1}{2}\delta_u\langle I_u^2\rangle k_c}{(k_c + \frac{1}{2}\delta_u\langle I_u^2\rangle)k_e}[CCa^{2+}]_0 \qquad (16)$$

where it is assumed that cage-calcium molecules in the center of the focal volume ($[CCa^{2+}(0, 0; t)]$ in Eq. 14) are replenished from and can escape into the surroundings with a characteristic diffusion rate of $k_c = 1.2D_{cg}/w_r^2$, where D_{cg} is the diffusion coefficient of calcium-bound cage molecules. The introduction of calcium buffers into this steady-state calculation is problematic, and consequently this equation cannot generally be applied to azid-1 because of the strong buffering capacity of the calcium-free cage that usually accompanies its use.

CONCLUSION

These action cross sections and calculations provide the tools required to use TPE of calcium cages for the quantitative release of calcium in regions as small as 1 fl. With the two-photon action cross sections given for azid-1 and DM-nitrophen, and the aforementioned calculations, it is now

possible to predict the amount of calcium released in a given MPE uncaging experiment and to predict the duration of the resultant calcium elevation.

Using ~7 mW of average power for a pulse train 10 μs in duration, 700-nm light overfilling a 1.3 NA objective can completely photolyze the calcium cage azid-1 contained within the 2PE focal volume. DM-nitrophen requires ~74 mW at its peak excitation wavelength of 730 nm to accomplish the same extent of photolysis, a power level that is more likely to lead to cellular photodamage than the ~7 mW required for azid-1. The resultant highly localized elevations in free calcium concentration will have durations that vary depending upon the diffusion times of the released ions and the local buffering conditions. In buffer free cytoplasm, the calcium distribution generated with a high (1.33) NA objective would last for ~165 μs (FWHM). This duration can be significantly extended by increasing the spatial extent of release and can be significantly reduced by the addition of calcium buffering agents.

These experiments and calculations demonstrate that 2PE of calcium cages should prove to be a useful method for three-dimensionally resolved calcium release in a variety of studies of cellular processes involving calcium.

This work was carried out at the Developmental Resource for Biophysical Imaging and Optoelectronics, with funding provided by the National Science Foundation (NSF) (grant DIR 88002787) and the National Institutes of Health (NIH) (grants RR07719 and RR04224). EBB was supported as a predoctoral trainee under NIH grant T32GM08267. JBS was supported as an NSF postdoctoral fellow under grant CHE-9403174. SRA and RYT were supported under grant number NS27177 and thank the Howard Hughes Medical Institute for support.

REFERENCES

Adams, S. R., V. Lev-Ram, and R. Y. Tsien. 1997. A new caged Ca^{2+}, azid-1, is far more photosensitive than nitrobenzyl-based chelators. *Chem. Biol.* 4:867–878.

Allbritton, N. L., T. Meyer, and L. Stryer. 1992. Range of messenger action of calcium ion and inositol-1,2,5-trisphosphate. *Science.* 258: 1812–1815.

Augustine, G. J., and E. Neher. 1992. Neuronal Ca^{2+} signaling takes the local route. *Curr. Opin. Neurobiol.* 2:302–307.

Cheng, H., W. J. Lederer, and M. B. Cannell. 1993. Calcium sparks: elementary events underlying excitation-contraction coupling in heart muscle. *Science.* 262:740–744.

Denk, W. 1994. Two-photon scanning photochemical microscopy: mapping ligand-gated ion channel distributions. *Proc. Natl. Acad. Sci.* 91: 6629–6633.

Denk, W., D. Piston, and W. Webb. 1995. Two-photon molecular excitation in laser-scanning microscopy. *In* Handbook of Biological Confocal Microscopy. J. Pawley, editor. Plenum Press, New York. 445–457.

Draajer, A., R. Sanders, and H. Gerritsen. 1995. Fluorescence lifetime imaging, a new tool in confocal microscopy. *In* Handbook of Biological Confocal Microscopy. J. Pawley, editor. Plenum Press, New York. 491–505.

Ellis-Davies, G. C. R., and J. H. Kaplan. 1994. Nitrophenyl-EGTA, a photolabile chelator that selectively binds Ca^{2+} with high affinity and releases it rapidly upon photolysis. *Proc. Natl. Acad. Sci. USA.* 91: 187–191.

Ellis-Davies, G. C. R., J. H. Kaplan, and R. J. Barsotti. 1996. Laser photolysis of caged calcium: rates of calcium release by nitrophenyl-EGTA and DM-nitrophen. *Biophys. J.* 70:1006–1016.

Escobar, A., P. Velez, A. Kim, F. Cifuentes, M. Fill, and J. Vergara. 1997. Kinetic properties of DM-nitrophen and calcium indicators: rapid transient response to flash photolysis. *Eur. J. Physiol.* 434:615–631.

Forsén, S., S. Linse, E. Thulin, B. Lindegård, S. Martin, P. Bayley, P. Brodin, and T. Grundström. 1988. Kinetics of calcium binding to calbindin mutants. *Eur. J. Biochem.* 177:47–52.

Kao, J. P. Y., and S. R. Adams. 1993. Photosensitive caged compounds: design, properties, and biological applications. *In* Optical Microscopy: Emerging Methods and Applications. B. Herman and J. L. Masters, editors. Academic Press, London. 27–85.

Kao, J. P. Y., and R. Y. Tsien. 1988. Calcium binding kinetics of fura-2 and azo-1 from temperature-jump relaxation measurements. *Biophys. J.* 53: 635–640.

Kaplan, J. H. 1990. Photochemical manipulation of divalent cation levels. *Annu. Rev. Physiol.* 52:897–914.

Kaplan, J. H., and G. C. R. Ellis-Davies. 1988. Photolabile chelators for the rapid photorelease of divalent cations. *Proc. Natl. Acad. Sci. USA.* 85:6571–6575.

Klein, M. G., H. Cheng, L. F. Santana, Y. H. Jiang, W. J. Lederer, and M. F. Schneider. 1996. Two mechanisms of quantized calcium release in skeletal muscle. *Nature.* 379:455–458.

Klingauf, J., and E. Neher. 1997. Modeling of buffered Ca^{2+} diffusion near the membrane: implications for secretion in neuroendocrine cells. *Biophys. J.* 72:674–690.

Lipp, P., C. Luscher, and E. Niggli. 1996. Photolysis of caged compounds characterized by ratiometric confocal microscopy: a new approach to homogeneously control and measure the calcium concentration in cardiac myocytes. *Cell Calcium.* 19:255–266.

Lipp, P., and E. Niggli. 1998. Fundamental calcium release events revealed by two-photon excitation photolysis of caged calcium in guinea pig cardiac myocytes. *J. Physiol.* 508:801–809.

Martin, S., S. Linse, C. Johansson, P. Bayley, and S. Forsen. 1990. Protein surface charges and Ca binding to individual sites in calbindin D9k: stopped flow studies. *Biochemistry.* 29:4188–4193.

McCray, J. A., N. Fidler-Lim, G. Ellis-Davies, and J. Kaplan. 1992. Rate of release of Ca^{2+} following laser photolysis of the DM-nitrophen-Ca^{2+} complex. *Biochemistry.* 31:8856–8861.

McCray, J. A., and D. R. Trentham. 1989. Properties and uses of photoreactive caged compounds. *Annu. Rev. Biophys. Biophys. Chem.* 18: 239–270.

Mertz, J., C. Xu, and W. Webb. 1995. Single-molecule detection by two-photon-excited fluorescence. *Optics Lett.* 20:2532–2534.

Naraghi, M. 1997. T-jump study of calcium binding kinetics of calcium chelators. *Cell Calcium.* 22:255–268.

Nelson, M. T., H. Cheng, M. Rubart, L. F. Santana, A. D. Bonev, H. J. Knot, and W. J. Lederer. 1995. Relaxation of arterial smooth muscle by calcium sparks. *Science.* 270:633–637.

Robinson, R., and R. Stokes. 1959. Electrolyte Solutions, the Measurement and Interpretation of Conductance, Chemical Potential, and Diffusion in Solutions of Simple Electrolytes. Butterworths Scientific Publications, London.

Shear, J., E. Brown, S. Adams, R. Tsien, and W. Webb. 1996. Two-photon excited photorelease of caged calcium. *Biophys. J.* 70:A211.

Stern, M. D. 1992. Buffering of calcium in the vicinity of a channel pore. *Cell Calcium.* 13:183–192.

Williams, B. M. 1997. One, two, and three photon excitation in laser scanning fluorescence microscopy: live cell measurements of phosopholipase hydrolysis, serotonin release and calcium sparks. PhD. thesis. Cornell University, Ithaca, NY.

Xu, C., and W. Webb. 1997. Multiphoton excitation of molecular fluorophores and nonlinear laser microscopy. *In* Topics in Spectroscopy, Vol. 5, Nonlinear and Two-Photon Induced Fluorescence. J. Lackowicz, editor. Plenum Press, New York. 471–540.

Xu, T., M. Naraghi, H. Kang, and E. Neher. 1997. Kinetic studies of Ca^{2+} binding and Ca^{2+} clearance in the cytosol of adrenal chromaffin cells. *Biophys. J.* 73:532–545.

Zhou, Z., and E. Neher. 1993. Mobile and immobile calcium buffers in bovine adrenal chromaffin cells. *J. Physiol.* 469:245–273.